Interactions of the Products, 8-Oxo-dGMP, dGMP, and Pyrophosphate with the MutT Nucleoside Triphosphate Pyrophosphohydrolase†

Vibhor Saraswat,‡ Michael A. Massiah,‡ Gregory Lopez,§ L. Mario Amzel,§ and Albert S. Mildvan*,‡

Department of Biological Chemistry and Department of Biophysics and Biophysical Chemistry, The Johns Hopkins School of Medicine, 725 North Wolfe Street, Baltimore, Maryland 21205-2185

Received August 26, 2002; Revised Manuscript Received October 2, 2002

ABSTRACT: The MutT enzyme from *E. coli*, in the presence of a divalent cation, catalyzes the hydrolysis of nucleoside- and deoxynucleoside-triphosphate (NTP) substrates by nucleophilic substitution at Pβ, to yield a nucleotide (NMP) and PPi. The best substrate of MutT is believed to be the mutagenic nucleotide 8-oxo-dGTP, on the basis of its $10^{3.4}$-fold lower K_m than that of dGTP (Maki, H., and Sekiguchi, M. (1992) *Nature 355*, 273−275). To determine the true affinity of MutT for an 8-oxo-nucleotide and to elucidate the kinetic scheme, product inhibition by 8-oxo-dGMP and dGMP and direct binding of these nucleotides to MutT were studied. With Mg^{2+}-activated dGTP hydrolysis, 8-oxo-dGMP is a noncompetitive inhibitor with $K_I^{slope} = 49$ nM, which is $10^{4.6}$-fold lower than the $K_I^{slope}$of dGMP (1.7 mM). Similarly, the $K_I^{intercept}$ of 8-oxo-dGMP is $10^{4.0}$-fold lower than that of dGMP. PPi is a linear uncompetitive inhibitor, suggesting that it dissociates first from the product complex, followed by the nucleotide. Noncompetitive inhibition by dGMP and 8-oxo-dGMP indicates an "iso" mechanism in which the nucleotide product leaves an altered form of the enzyme which slowly reverts to the form which binds substrate. Consistent with this kinetic scheme, $^1H-^{15}N$ HSQC titration of MutT with dGMP reveals weak binding and fast exchange from one site with a $K_D = 1.8$ mM, in agreement with its K_I^{slope}. With 8-oxo-dGMP, tight binding and slow exchange ($n = 1.0 \pm 0.1$, $K_D < 0.25$ mM) are found. Isothermal calorimetric titration of MutT with 8-oxo-dGMP yields a K_D of 52 nM, in agreement with its K_I^{slope}. Changing the metal activator from Mg^{2+} to Mn^{2+} had little effect on the K_I^{slope} of dGMP or of 8-oxo-dGMP, consistent with the second-sphere enzyme$-M^{2+}-H_2O-$NTP$-M^{2+}$ complex found by NMR (Lin, J., Abeygunawardana, C., Frick, D. N., Bessman, M. J., and Mildvan, A. S. (1997) *Biochemistry 36*, 1199−1211), but it decreased the K_I of PPi 12-fold, suggesting direct coordination of the PPi product by the enzyme-bound divalent cation. The tight binding of 8-oxo-dGMP to MutT ($\Delta G° = -9.8$ kcal/mol) is driven by a highly favorable enthalpy ($\langle \Delta H_{binding} \rangle = -32 \pm 7$ kcal/mol), with an unfavorable entropy ($\langle -T\Delta S°_{binding} \rangle = +22 \pm 7$ kcal/mol), as determined by van't Hoff analysis of the effect of temperature on the K_I^{slope} and by isothermal titration calorimetry in two buffer systems. The binding of 8-oxo-dGMP to MutT induces changes in backbone ^{15}N and NH chemical shifts of 62 residues widely distributed throughout the protein, while dGMP binding induces smaller changes in only 22 residues surrounding the nucleotide binding site, suggesting that the unusually high affinity of MutT for 8-oxo-nucleotides is due not only to interactions with the altered 8-oxo or 7-NH positions on guanine, but results primarily from diffuse structural changes which tighten the protein structure around the 8-oxo-nucleotide.

The MutT enzyme from E. coli (129 residues) is a prototypical Nudix hydrolase[1] (*1*), which catalyzes the unusual hydrolysis of nucleoside- and deoxynucleoside-triphosphate (NTP) substrates, by nucleophilic substitution at the rarely attacked Pβ, to yield a nucleotide (NMP) and pyrophosphate (PPi) (eq 1) (*2*, *3*):

$$NTP + H_2O \rightarrow NMP + PPi + H^+ \qquad (1)$$

The enzyme requires two divalent cations for activity, one coordinated directly to the protein and the other coordinated to the β- and γ-phosphoryl groups of the NTP substrate (*4*). A mechanism has been proposed (Figure 1), on the basis of the solution structure of the MutT$-Mg^{2+}-(H_2O)-$AMPCPP$-Mg^{2+}$ complex (*5*), and the effects of mutations on the hydrolysis of dGTP and on metal binding by the enzyme (*6*). In this mechanism, an inner-sphere water ligand of the enzyme-bound divalent cation, assisted by Glu-53, attacks the β-phosphorus of $M^{2+}-$NTP, displacing the NMP leaving group which dissociates from the enzyme. The remaining

† This research was supported by National Institutes of Health Grant DK28616 (to A.S.M.). G.L. was supported by National Institutes of Health Grant A149485 (to L.M.A.)

* To whom correspondence should be addressed. Phone: 410-955-2038. Fax: 410-955-5759. E-mail: mildvan@welchlink.welch.jhu.edu.

‡ Department of Biological Chemistry.

§ Department of Biophysics and Biophysical Chemistry.

[1] Abbreviations: 8-oxo-dGMP, 8-oxo-deoxyguanosine monophosphate; HEPES, 4-(2-hydroxyethyl)-1-piperazineethanesulphonic acid; HSQC, heteronuclear single quantum coherence; ITC, isothermal titration calorimetry; NOESY, nuclear Overhauser effect spectroscopy; NMP, nucleoside monophosphate; NTP, nucleoside triphosphate; Nudix hydrolase, **nu**cleoside **di**phosphate-**X** hydrolase; PPi, pyrophosphate; TOCSY, total correlation spectroscopy.

10.1021/bi020552p CCC: $22.00
Published on Web 12/05/2002

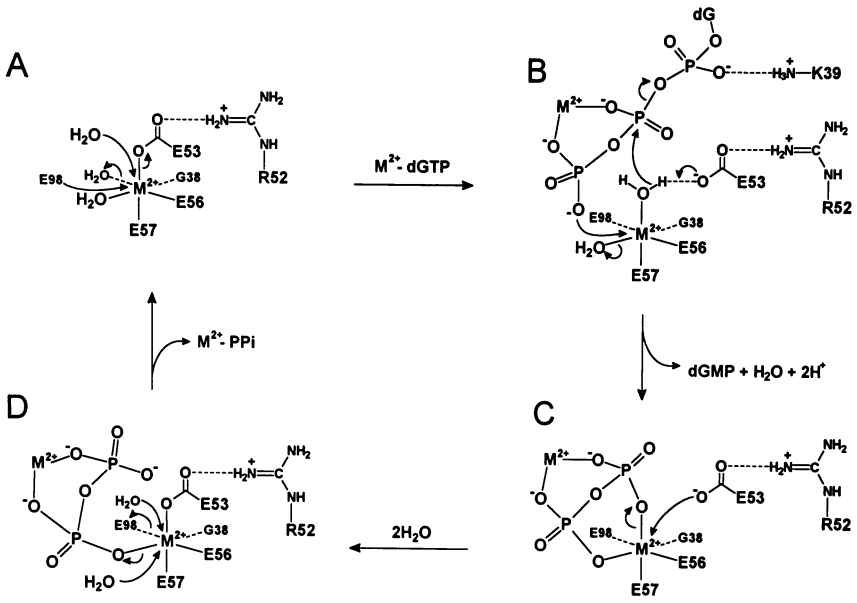

FIGURE 1: Proposed mechanism of the MutT reaction based on structural (*5*) and mutagenesis studies (*6*).

PPi product, now in an inner-sphere enzyme−M^{2+}−PPi−M^{2+} complex, dissociates from the enzyme, displaced by Glu-53 which enters the coordination sphere of the enzyme-bound divalent cation. In the next catalytic cycle, Glu-53 dissociates from the bound metal to activate the attacking water. While consistent with structural and binding studies, this mechanism has not been thoroughly tested kinetically, and alternative reaction sequences have not been ruled out (*6*).

The best substrate of the MutT enzyme in vitro is 8-oxo-dGTP with a K_m which is $10^{3.4}$-fold lower (0.48 μM) than that of dGTP (1100 μm) but with the same k_{cat} (4 s^{-1}) (*7*). These observations are consistent with the proposed biological role of MutT (*7*), since 8-oxo-dGTP is a mutagenic nucleotide in vitro which mispairs with template adenine during DNA replication (*8*, *9*). MutT deficient *E. coli* show a 10^4-fold increase in mutations, all of which are AT → CG transversions (*10*, *11*). Homologous 8-oxo-dGTPases have been found in mouse (*12*) and human cell lines (*13*). Both male and female mice in which the MutT gene has been inactivated show major increases in the occurrence of tumors at 18 months of age (*14*). It has therefore been proposed that the mutagenic phenotype of MutT deficient cells results from in vivo mispairing of 8-oxo-dGTP, derived from oxidative damage to guanine nucleotides, with template adenine during DNA replication (*7*, *14*). This hypothesis is controversial because of the low levels of 8-oxo-dGTP detected in MutT$^-$ *E. coli*, leaving open the possibility that other mutagenic nucleotides are the actual in vivo substrates of the MutT enzyme (*15*).

Despite uncertainties about the in vivo substrate of MutT, 8-oxo-dGTP is by far the best in vitro substrate, on the basis of its low K_m. The structure of 8-oxo-dGTP differs from that of dGTP by a C═O instead of a C−H at position 8 of the purine ring, and an N−H instead of an N at position 7. The $10^{3.4}$-fold lower K_m of 8-oxo-dGTP compared to that of dGTP (*7*) is not readily explained by the solution structure of the MutT−Mg^{2+}−AMPCPP−Mg^{2+} complex, which can accommodate the structural enlargements in 8-oxo-dGTP but which shows no specific interactions with them (*5*).

In this paper, we have tested, independently of K_m values, whether an 8-oxo-guanine nucleotide actually does bind more tightly to MutT than does the corresponding guanine nucleotide by kinetic, NMR, and calorimetric methods. A preliminary abstract of this work has been published (*16*).

EXPERIMENTAL PROCEDURES

Materials. The construction of the plasmid pETMutT, containing the mutT gene under control of the T7 promoter (pET system, Novagen Inc., Madison, WI), has been described previously (*17*). The isopropyl β-D-thiogalactoside (IPTG) was from Roche (Indianapolis, IN). Tryptone and yeast extract were obtained from Difco (Detroit, MI). Ammonium sulfate, ampicillin, 2′-deoxyguanosine 5′-monophosphate, 2′-deoxyguanosine 5′-diphosphate, 2′-deoxyguanosine 5′-triphosphate, dithiothreitol (DTT), lysozyme, and streptomycin sulfate were from Sigma (St. Louis, MO). Vivaspin (MWCO 5000) centrifugal concentrators were purchased from Vivascience Limited (Gloucestershire, U.K.). The Mono Q column (HR 5/5), Sephadex G-100 and DEAE-Sepharose fast-flow were from Pharmacia Biotech (Piscataway, NJ). The Microsorb 300-5 C18 HPLC column was from Dynamax-Rainin (Woburn, MA). Deuterium oxide (D_2O 99.96% D) was from Aldrich (Milwaukee, WI). Uniformly (99%) ^{15}N-enriched $^{15}NH_4Cl$ and uniformly (99%) ^{13}C-enriched D-glucose were from Isotech Inc. (Miamisburg, OH). [γ-^{32}P]ATP (4×10^6 Ci/mol) and EcoLite (+) scintillation cocktail were from ICN Biomedicals Inc. (Costa Mesa, CA). All solvents and reagents were of the highest purity available, and buffers were treated with Chelex-100 before use to remove trace metals.

Preparation of MutT. The recombinant *E. coli* strain HMS174(DE3)[pETMutT] was used for production of unlabeled, uniformly ^{15}N-labeled, and uniformly ^{13}C- and ^{15}N-labeled MutT (*17*). The enzyme was purified to >95% homogeneity on the basis of SDS−PAGE and specific activity (500 IU/mg) as described (*6*).

Synthesis and Purification of 8-oxo-dGMP. 8-oxo-dGMP was synthesized by a modification of the procedure of Mo

et al. (*13*), by incubating 6 mM dGMP in 100 mM sodium phosphate buffer, pH 6.8, 30 mM ascorbic acid, and 100 mM hydrogen peroxide in the dark at 37 °C for 3 h. Aliquots of this crude 8-oxo-dGMP were stored at −80 °C. When needed, an aliquot was thawed and filtered through a 0.22 micron syringe filter and loaded on to a Mono Q anion exchange column in an FPLC system (Pharmacia Biotech). The elution was done with a 0.5−15% linear concentration gradient of triethylammonium bicarbonate buffer (1M, pH 8.0) at 4 °C. The identification of the 8-oxo-dGMP peak was confirmed by UV spectroscopic scanning on a Beckman DU 640 spectrophotometer (200−320 nm), which showed characteristic maxima at 247 and 293 nm with extinction coefficients 1.230×10^4 M^{-1} cm^{-1} and 1.496×10^4 M^{-1} cm^{-1}, respectively (*18*−*20*). The pooled fractions were concentrated by freeze-drying to 1 mM concentration and loaded on to a C18 column in a Dynamax-Rainin HPLC system. The 8-oxo-dGMP peak monitored by UV absorption at 260 nm was isocratically eluted at 25 °C with a buffer containing 12.5 mM citric acid, 25 mM sodium acetate, 10 mM acetic acid, and 30 mM NaOH (final concentrations). The pH was adjusted to 5.4 with NaOH. The collected fractions of 8-oxo-dGMP were concentrated by freeze-drying to 1mM. Samples thus prepared were loaded again on the Mono Q column and eluted as mentioned above in order to change the buffer to triethylammonium bicarbonate. The fractions thus obtained were pooled and concentrated by freeze-drying. The dried sample of pure 8-oxo-dGMP was dissolved in distilled water, its pH was adjusted to 7.5 with 0.5 M HCl, and its molecular mass (363.2 Da) and purity (≥98%) were confirmed by electrospray ionization mass spectrometry. The 500 MHz ^{1}H NMR spectrum in 99.9% D_2O showed no aromatic resonances but did show deoxyribose resonances, consistent with those previously reported (*18*). The purity of the 8-oxo-dGMP thus prepared was further checked by analytical C18 HPLC, which yielded a single peak of ≥95% purity with the UV spectral properties described above.

General Methods. The concentration of MutT was determined spectrophotometrically using $A_{280}^{1mg/mL}$ of 2.2 (*4*). Concentrations of dGTP solutions were determined using the extinction coefficient, ϵ_{252} of 1.37×10^4 M^{-1} cm^{-1} (4). Concentrations of 8-oxo-dGMP were measured using the extinction coefficient, ϵ_{293} of 1.496×10^4 M^{-1} cm^{-1} (*20*).

Kinetic Studies. [γ-^{32}P]dGTP was prepared by transphosphorylation of dGDP with [γ-^{32}P]ATP as previously reported (*6*). Steady-state kinetic experiments with Mg^{2+} or Mn^{2+} activated MutT were performed by measuring the amount of [γ-^{32}P]pyrophosphate released from [γ-^{32}P]dGTP in Tris-HCl buffer (50 mM, pH 7.5) at 23 °C (*4*, *6*, *21*). After quenching the reaction with 0.5 M $HClO_4$ and 20% charcoal the suspension was incubated for 5 min at 2 °C and centrifuged. The supernatant (30 μL) was dissolved in Ecolite scintillation cocktail (3.5 mL) and counted in a Beckman LS 6000SE automatic liquid scintillation counter. The kinetic data were analyzed by two independent methods that yielded the same inhibitor constants within experimental error: (i) nonlinear least-squares fitting of the primary kinetic data to hyperbolic functions relating initial velocity to substrate concentration followed by linear least-squares fitting of computed slopes and intercepts versus inhibitor concentration and (ii) nonlinear least-squares fitting of the total kinetic data to the global rate equation (eq 4, Results). The inhibitor constants are reported ± the standard deviation. Linear and nonlinear regression analyses were performed using the program Grafit (Erithacus Software Ltd., Staines, U.K.).

^{1}H−^{15}N HSQC Spectral Titrations of MutT with Ligands. ^{1}H−^{15}N HSQC titrations of MutT with dGMP or 8-oxo-dGMP were carried out with samples containing ^{15}N-labeled wild-type MutT (0.75 mM in dGMP titrations and 0.25 mM in 8-oxo-dGMP titrations), 4 mM d_{11}-Tris-HCl buffer (pH 7.5), 21 mM NaCl, 15 mM $MgCl_2$, 0.33 mM sodium azide, and 10% D_2O in a total volume of 580 μL. To maintain a constant level of free Mg^{2+} at high nucleotide concentrations, stoichiometric $MgCl_2$ was added together with the nucleotide, when necessary. The NMR data were collected at 23 °C on a Varian Unityplus 600 MHz NMR spectrometer equipped with *z*-axis pulsed field gradient capabilities, using a Varian 5 mm triple resonance probe. Data were collected using the pulse sequence previously described (*22*) and processed on a Silicon Graphics Octane Workstation using NMRPipe (*23*). At each nucleotide concentration, the intensities of the protein ^{15}N−^{1}H cross-peaks were measured using the NMRVIEW 2.1 software package (*24*). In the dGMP titrations, the dissociation constant (K_D) of dGMP from the MutT−Mg^{2+} complex was obtained by measuring the chemical shift changes of six amino acid residues under conditions of fast exchange, and fitting the titration data to eq 2 by nonlinear least-squares regression analysis with the program Grafit:

$$\Delta\delta_{obs} = [\Delta\delta_{max}/2E_t]\,[(K_D + L_t + E_t) - \{(K_D + L_t + E_t)^2 - 4L_tE_t\}^{1/2}] \quad (2)$$

In eq 2, L_t is the total dGMP concentration, E_t is the total enzyme concentration (taking into account the small changes in enzyme concentration due to dilution on adding dGMP), $\Delta\delta_{obs}$ is the observed chemical shift change, and $\Delta\delta_{max}$ is the chemical shift change at saturating dGMP (*6*).

In the 8-oxo-dGMP titrations, which showed slow exchange on the NMR time scale, the decreasing intensities of 28 amino acid residues were plotted versus the relative concentrations of 8-oxo-dGMP and MutT and analyzed by linear least-squares regression analysis to determine the stoichiometry of 8-oxo-dGMP binding. Because the dissociation constant of 8-oxo-dGMP from the Mg^{2+}−enzyme was much lower than the required enzyme concentration (0.25 mM), only the binding stoichiometry and an upper limit to K_D could be determined from these titrations. The chemical shifts of the backbone ^{15}N and NH resonances of MutT in the 8-oxo-dGMP complex were sequence specifically assigned by analysis of ^{15}N-edited TOCSY (*25*, *26*) and NOESY experiments with ^{15}N-labeled enzyme (*27*), as well as HNCA (*28*) and CBCACONH (*29*) triple resonance experiments with ^{13}C- and ^{15}N-labeled enzyme.

Isothermal Titration Calorimetry. ITC experiments were performed with an Omega calorimeter (*30*) manufactured by Microcal, Inc., Northampton, MA, at 18 ± 0.2, 23 ± 0.2, and 28 ± 0.2 °C. In these experiments, typically, 10 injections of 10 μL of either 123.5 or 110.0 μM 8-oxo-dGMP were titrated into 1.8 mL of an approximately 6 μM solution of MutT. Heats of dilution of 8-oxo-dGMP, measured by titrating the nucleotide into buffer, were subtracted from the MutT titration data. The data were processed using Origin

2.9 (Microcal, Inc., Northampton, MA) using the model of a single set of noninteracting sites. During the fit, the stoichometry of binding was set to 1, as found by NMR titration, and the concentration of functional MutT was corrected to account for this.

Experiments were done in two buffers with different heats of ionization to account for the change in protonation state upon binding: either 50 mM Tris−HCl or 50 mM HEPES containing 15 mM $MgCl_2$ at pH 7.5. In any given calorimetric binding experiment, the measured enthalpy, after correction for dilution, consists of heat due to binding and heat due to change in protonation state of the buffer:

$$\Delta H_{\text{experimental}} = \Delta H_{\text{binding}} + \Delta n \Delta H_{\text{ionization}} \qquad (3)$$

where $\Delta H_{\text{experimental}}$ is the experimentally determined enthalpy of the binding experiment, $\Delta H_{\text{binding}}$ is the enthalpy of binding corrected for buffer effects, but including the intrinsic enthalpy of binding and the ionization enthalpies of the protein and ligand, Δn is the number of protons gained or lost by the buffer during the binding event, and $\Delta H_{\text{ionization}}$ is the enthalpy of ionization of the buffer. From measurements of the experimental enthalpy of binding ($\Delta H_{\text{experimental}}$) in two different buffers, eq 3 can be solved for both Δn and $\Delta H_{\text{binding}}$.

RESULTS AND DISCUSSION

Inhibition of Mg^{2+}-Activated MutT by 8-oxo-dGMP and dGMP. Studies of product inhibition are often useful in elucidating product affinities and reaction mechanisms (*31*−*34*). As an independent test of the unusually high affinity of the MutT enzyme for 8-oxo-guanine nucleotides, suggested by the low K_m of the substrate 8-oxo-dGTP (*7*), we studied inhibition by the product of its MutT catalyzed reaction, 8-oxo-dGMP. For comparison we used dGMP as a control inhibitor so that we could clarify the roles of the structural alterations of the guanine ring in nucleotide binding to MutT. For the kinetic experiments, 8-oxo-dGMP was synthesized and purified as described in Experimental Procedures. The effects of 8-oxo-dGMP and dGMP on the initial velocities of the MutT-catalyzed hydrolysis of Mg^{2+}−dGTP were studied by varying the substrate concentration at a fixed and saturating concentration of free $MgCl_2$, and at four fixed inhibitor concentrations.

Double reciprocal plots show that 8-oxo-dGMP acts as a noncompetitive inhibitor[2] of MutT (Figure 2A), affecting both the apparent V_{max} and the apparent K_m of Mg^{2+}−dGTP. Self-consistent results were found in five such experiments. To further characterize the data, they were analyzed by secondary plots. Both the slopes and intercepts of the double reciprocal plots as a function of 8-oxo-dGMP concentration give straight lines (Figure 2B,C) confirming the linear noncompetitive inhibition of MutT by 8-oxo-dGMP in the presence of Mg^{2+}. Secondary plots from these experiments were used to calculate the values of K_I^{slope} and $K_I^{intercept}$, which are summarized in Table 1. Independent analyses of the total kinetic data by nonlinear least-squares fitting to the global rate equation (see eq 4 below) yielded the same inhibitor constants, within experimental error. The errors are reported as standard deviations in Table 1.

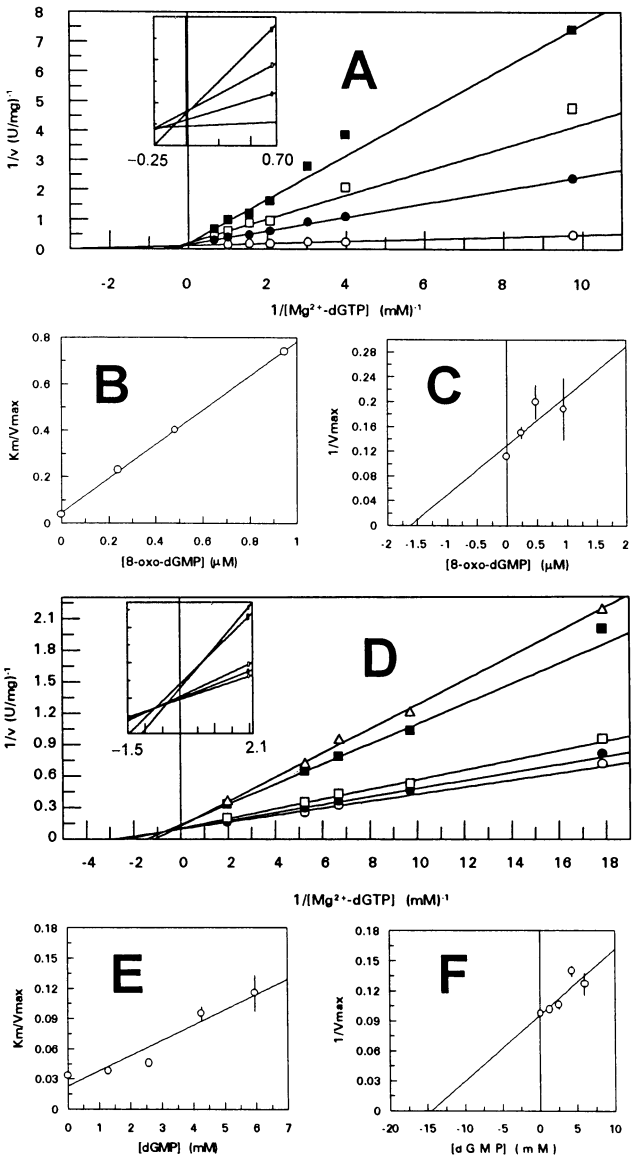

FIGURE 2: MutT inhibition by 8-oxo-dGMP and dGMP with Mg^{2+} as the activator. (A) Double reciprocal plot of initial velocity against Mg^{2+}−dGTP concentration at 16 mM $MgCl_2$, 50 mM Tris−HCl (pH 7.5), at 23 °C, and the following 8-oxo-dGMP concentrations: 0.0 (○), 0.24 (●), 0.48 (□), and 0.95 μM (■). (B) Secondary plot of the slope (K_m/V_{max}) vs 8-oxo-dGMP concentration. (C) Secondary plot of the intercept ($1/V_{max}$) vs 8-oxo-dGMP concentration. (D) Double reciprocal plot of initial velocity against Mg^{2+}−dGTP concentration at 16 mM $MgCl_2$ and the following dGMP concentrations: 0.0 (○), 1.28 (●), 2.58 (□), 4.26 (■), and 5.96 mM (△). Other components and conditions are as given in Figure 2A. (E) Secondary plot of the slope (K_m/V_{max}) vs dGMP concentration. (F) Secondary plot of the intercept ($1/V_{max}$) vs dGMP concentration. Insets in A and D expand the region around the $1/v$ axis.

As found with 8-oxo-dGMP, noncompetitive inhibition by dGMP was also found (Figure 2D) with linear secondary plots (Figure 2E,F) in two experiments. The binding of 8-oxo-dGMP was $10^{4.6}$ and $10^{4.0}$ times tighter than the binding of dGMP on the basis of K_I^{slope} and $K_I^{intercept}$ values, respectively (Table 2), although $K_I^{intercept}$ contains kinetic terms as well (see below).

Effect of Temperature on the Thermodynamic and Kinetic Parameters of Mg^{2+}-Activated MutT. The unusually high

[2] Noncompetitive inhibition and mixed-type inhibition are synonymous (*32*).

Table 1: Product Inhibition of the MutT-Catalyzed Hydrolysis of dGTP at 23° C, pH 7.5

inhibitor	activator	type of inhibition	K_I^{slope} (μM)	$K_I^{intercept}$ (μM)
8-oxo dGMP	Mg^{2+}	noncompetitive	0.049 ± 0.015	1.620 ± 0.880
dGMP	Mg^{2+}	noncompetitive	1740 ± 490	14500 ± 5420
8-oxo dGMP	Mn^{2+}	noncompetitive	0.173 ± 0.025	0.593 ± 0.160
dGMP	Mn^{2+}	noncompetitive	3960 ± 291	4570 ± 134
PPi	Mg^{2+}	uncompetitive	−	4950 ± 1700
PPi	Mn^{2+}	uncompetitive	−	413 ± 70

Table 2: Comparison of Product Inhibition by 8-oxo-dGMP and dGMP

activator	K_I^{slope} (dGMP) / K_I^{slope} (8-oxo-dGMP)	$K_I^{intercept}$ (dGMP) / $K_I^{intercept}$ (8-oxo-dGMP)
Mg^{2+}	$10^{4.6}$	$10^{4.0}$
Mn^{2+}	$10^{4.4}$	$10^{3.9}$

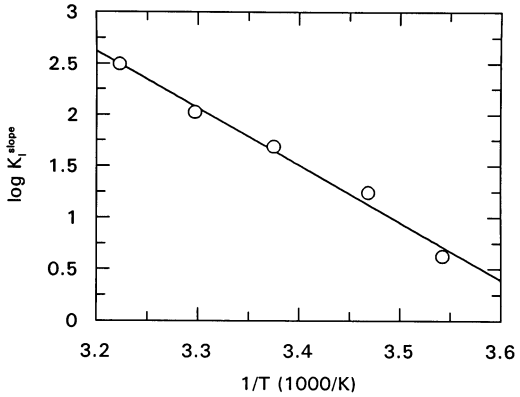

FIGURE 3: Temperature dependence of K_I^{slope}. The K_I^{slope} values were determined at 4, 14, 23, 29, and 37 °C. The pH of Tris−HCl buffer (50 mM) was adjusted to 7.5 at each temperature. Other reaction components and conditions were as given in Figure 2.

affinity of MutT for 8-oxo-dGMP as measured by K_I^{slope} corresponds to a free energy of binding of -9.8 ± 0.2 kcal/mol. To determine whether this large negative $\Delta G°_{binding}$ was driven by enthalpy or entropy, the values of K_I^{slope} for 8-oxo-dGMP were determined with the Mg^{2+} activated enzyme at 9, 15, 23, 30, and 37 °C, maintaining constant pH by adjusting the pH of the buffer at each temperature. Below 9 °C the measured reaction rates were too low to yield reliable values of K_I^{slope}. A van't Hoff plot of these data (Figure 3) yielded for $1/K_I^{slope}$ a very favorable $\Delta H_{binding}$ of -25.5 ± 4.1 kcal/mol, and an unfavorable $-T\Delta S°_{binding}$ of $+15.7 \pm 4.1$ kcal/mol (Table 3). Similar values of $\Delta H_{binding}$ of -26.5 ± 3.5 kcal/mol and $-T\Delta S°_{binding}$ of $+18.7 \pm 3.5$ kcal/mol were found for $1/K_I^{intercept}$ over the more limited temperature range of 9° to 30°C (Table 3). Large errors in extrapolation precluded the use of data outside of this temperature range. These results indicate that the thermodynamic driving force for the binding of 8-oxo-dGMP is enthalpic.

From the same experiments (Table 3), the temperature dependence of $1/K_m(Mg^{2+}-dGTP)$ yielded a favorable ΔH and an unfavorable $-T\Delta S°$ for substrate binding in the steady state. The temperature dependence of k_{cat} revealed the kinetic barrier to catalysis to be enthalpic, with a negligible entropic contribution (Table 3).

Inhibition of Mn^{2+}-Activated MutT by 8-oxo-dGMP and dGMP. Maintaining the same reaction conditions for the kinetics, care was taken to keep the concentration of free Mn^{2+} constant and saturating. As found with Mg^{2+}-activated MutT, double reciprocal plots of the kinetic data with Mn^{2+} activation (Figures S1 and S2, Supporting Information) indicate noncompetitive inhibition by 8-oxo-dGMP in four experiments, and by dGMP in two experiments. The secondary plots of slope and intercept show similar linear behavior as found with Mg^{2+}, and the K_I values are given in Table 1. In the presence of Mn^{2+} as activator, the binding of 8-oxo-dGMP to MutT ($K_I^{slope} = 0.173 \pm 0.025$ μM) was $10^{4.4}$ times tighter than the binding of dGMP, in good agreement with the ratio obtained with Mg^{2+} (Table 2). Similarly, the $K_I^{intercept}$ values of 8-oxo-dGMP and dGMP with Mn^{2+} suggest the tighter binding of 8-oxo-dGMP by a factor of $10^{3.9}$ as found with Mg^{2+} (Table 2), although $K_I^{intercept}$ contains kinetic terms as well (see below). Accordingly, as seen in Table 4, on changing the metal activator from Mn^{2+} to Mg^{2+} (which increases k_{cat} 21-fold (*4*)), the K_I^{slope} values of both dGMP and 8-oxo-dGMP show a small decrease, suggesting slightly greater affinity of the enzyme−Mg^{2+} complex for these nucleotides, while the $K_I^{intercept}$ values increase slightly. These small effects are consistent with the structure of the MutT−M^{2+}−H_2O−AMPCPP−M^{2+} complex which showed only indirect, second-sphere interactions of the nucleotide with the enzyme bound divalent cation (*5*).

Inhibition by Pyrophosphate. The inhibition of MutT by pyrophosphate was studied with Mg^{2+} and Mn^{2+} as activators. Double reciprocal plots with either Mg^{2+} (Figure 4A−C) or Mn^{2+} activation (Figure 4D−F) show that PPi is a

Table 3: Kinetic and Thermodynamic Parameters of MutT−Mg^{2+}−Nucleotide Complexes

kinetic parameter	units	value at 23 °C	thermodynamic parameter (kcal/mol) $\Delta G^‡$	$\Delta H^‡$	$-T\Delta S^‡$
k_{cat}	s^{-1}	2.1 ± 0.1	16.8 ± 0.1	14.8 ± 2.3	2.0 ± 2.3
			$\Delta G°_{binding}$	$\Delta H_{binding}$	$-T\Delta S°_{binding}$
$1/K_m$ (Mg^{2+}dGTP)	mM^{-1}	3.1 ± 0.3	-4.7 ± 0.1	-11.4 ± 2.0	6.7 ± 2.0
$1/K_I^{slope}$ (8-oxo-dGMP)	μM^{-1}	20.4 ± 6.3	-9.8 ± 0.2	-25.5 ± 4.1	15.7 ± 4.1
$1/K_I^{intercept}$ (8-oxo-dGMP)	μM^{-1}	0.62 ± 0.34	-7.8 ± 0.4	-26.5 ± 3.5	18.7 ± 3.5
$1/K_D$ (8-oxo-dGMP)[a]	μM^{-1}	19.2 ± 5.1	-9.8 ± 0.2	-39.0 ± 0.7	29.2 ± 0.7
$1/K_D$ (dGMP)	mM^{-1}	0.56 ± 0.04[b]	-3.7 ± 0.3[b]	-3.3 ± 0.3[a]	-0.4 ± 0.4[a,b]

[a] Determined by ITC. [b] Determined by $^1H-^{15}N$ HSQC titration.

Table 4: Effects of Activating Divalent Cation on the K_I Values of the Reaction Products

inhibitor	K_I^{slope} (with Mg^{2+}) / K_I^{slope} (with Mn^{2+})	$K_I^{intercept}$ (with Mg^{2+}) / $K_I^{intercept}$ (with Mn^{2+})
dGMP	0.44	3.17
8-oxo-dGMP	0.28	2.74
PPi	−	11.98

Scheme 1

$$E + S \rightleftharpoons ES \longrightarrow EPQ \rightleftharpoons EQ \rightleftharpoons E$$

Scheme 2

$$E + S \underset{k_2}{\overset{k_1}{\rightleftharpoons}} ES \underset{k_4}{\overset{k_3}{\rightleftharpoons}} EPQ \underset{k_6}{\overset{k_5}{\rightleftharpoons}} FQ \underset{k_8}{\overset{k_7}{\rightleftharpoons}} F \underset{k_{10}}{\overset{k_9}{\rightleftharpoons}} E$$

linear uncompetitive inhibitor. The $K_I^{intercept}$ of PPi in the presence of Mn^{2+} is 12-fold lower than that in the presence of Mg^{2+} (Table 4). Since polyphosphate ligands generally bind Mn^{2+} an order of magnitude more tightly than Mg^{2+} (*35*), these $K_I^{intercept}$ values suggest an important role played by the activating metal in the binding of the PPi product, to the enzyme, as proposed in Figure 1C. Alternatively, the decrease in $K_I^{intercept}$ of PPi with Mn^{2+} could have resulted from a kinetic effect, such as an increase in the rate constant of the chemical step (see below). However, this possibility is less likely, since k_{cat} with Mn^{2+} is 21-fold *lower* than with Mg^{2+} under these conditions (*4*), and the chemical step may contribute to k_{cat} (*6*).

Kinetic Scheme of the MutT Reaction. As seen in eq 1, the chemical step of the MutT pyrophosphohydrolase reaction is highly irreversible, and one of the two substrates is water, which is present at a high and constant concentration. Hence, to interpret the product inhibition data, we make the simplest, reasonable assumption that MutT catalyzes a Uni Bi reaction, with NTP as the substrate and NMP and PPi as products, which has an irreversible step in the catalytic segment (Scheme 1).

The rate equation for Scheme 1 predicts uncompetitive inhibition by P, the first product to leave, since P binds to a different form of the enzyme than S does, and competitive inhibition by Q, the second product to leave, since Q binds to the same form of the enzyme that S does (*31*−*34*). Experimentally, while inhibition by PPi is uncompetitive (Figure 4), indicating that PPi is the first product to leave, inhibition by dGMP or by 8-oxo-dGMP, is noncompetitive (Figures 2, S1, and S2 and Table 1). Hence, a more complicated reaction scheme (Scheme 2) is necessary to explain the observations that the nucleotide products, Q, compete at low substrate (to give a slope effect) and also inhibit at saturating substrate (to give an intercept effect). The simplest explanation is given in Scheme 2, in which the enzyme undergoes a conformational change from E to F during the reaction (k_5) which must be reversed in the free enzyme, in a partially rate-limiting step (k_9), before the next substrate molecule can bind (*31*−*34*, *36*, *37*).

In Scheme 2, k_4 is negligible because of the irreversible chemical step, and k_9 is much less than k_{10}. The slope effect of Q occurs at low substrate concentration, where most of the enzyme is free, because Q, by binding only to F, shifts the E ⇌ F equilibrium to F, while S, by binding only to E, shifts the E ⇌ F equilibrium to E. The intercept effect of Q arises because of the rate-limiting k_9 step in which F → E. Hence, at saturating S, virtually all of the enzyme is free, in the F form, which does not bind S. Such mechanisms involving partially rate-limiting steps which occur in the free enzyme are referred to as "iso" mechanisms (*31*−*34*, *36*, *37*). The observation that the preferred substrate of MutT, 8-oxo-dGTP with a $10^{3.4}$-fold lower K_m than dGTP has the

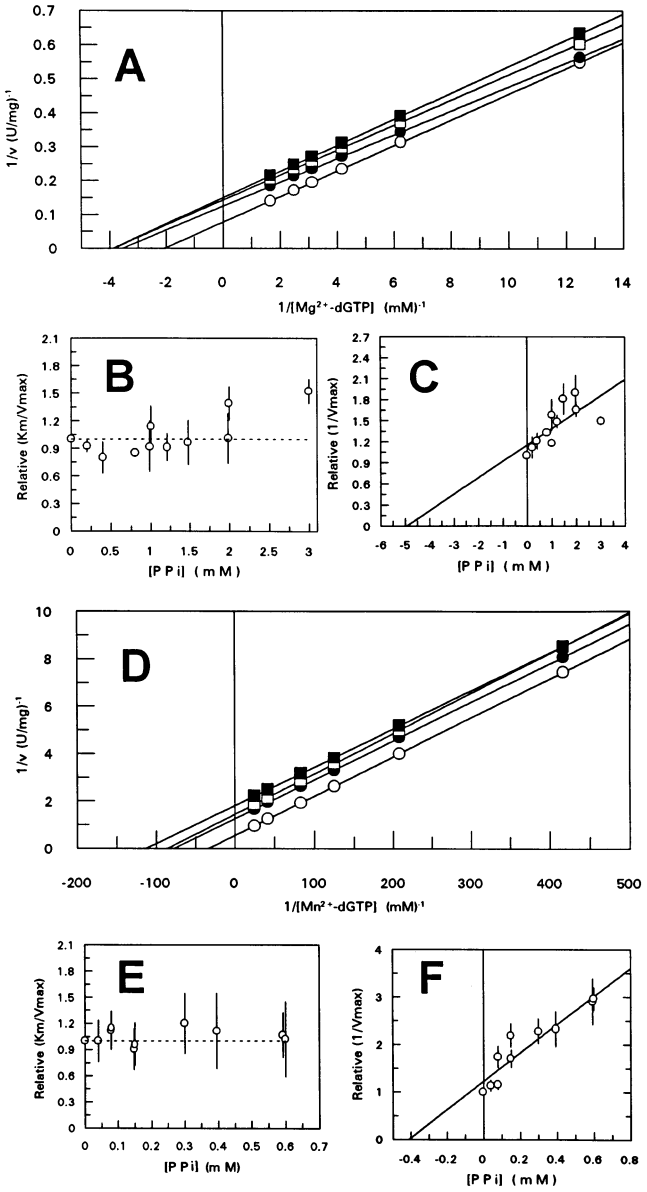

FIGURE 4: MutT inhibition by pyrophosphate. (A) Double reciprocal plot of initial velocity against Mg^{2+}−dGTP concentration at (12 + [PPi]) mM $MgCl_2$, 50 mM Tris−HCl (pH 7.5), 23 °C temperature, and the following PPi concentrations: 0.0 (○), 0.988 (●), 1.48 (□), and 1.98 mM (■). (B) Secondary plot of the slopes (K_m/V_{max}), relative to the uninhibited values in three experiments, vs PPi concentration. (C) Secondary plot of the intercepts ($1/V_{max}$), relative to the uninhibited values in three experiments, vs PPi concentration. (D) Inhibition by pyrophosphate of Mn^{2+}-activated MutT. Double reciprocal plot of initial velocity against Mn^{2+}−dGTP concentration at (2 + [8-oxo-dGMP]/3 + [dGTP]) mM $MnCl_2$, 50 mM Tris−Cl (pH 7.5), 23 °C, and the following PPi concentrations: 0.0 (○), 0.198 (●), 0.395 (□), and 0.593 mM (■). (E) Secondary plot of the slopes (K_m/V_{max}), relative to the uninhibited values in two experiments, vs PPi concentration. (F) Secondary plot of the intercepts ($1/V_{max}$), relative to the uninhibited values in two experiments, vs PPi concentration.

same k_{cat} (*7*), is consistent with an iso mechanism in which the F → E step is kinetically dominant.

A rate equation (eq 4) has been derived by the King-Altman method in terms of the individual rate constants of Scheme 2 (*33*, *34*):

$$v = V_f[S]/\{K_m + [S] + K_m[Q]/K_{IQ}^{slope} + [S][P]/K_{IP}^{int} + K_m[P][Q]/K_P K_{IQ}^{slope} + [S][Q]/K_{IQ}^{int} + [S][P][Q]/K_P K_{IQ}^{int}\} \quad (4)$$

In the absence of P, eq 4 shows noncompetitive inhibition by Q, with

$$K_{IQ}^{slope} = k_7/k_8(1 + k_9/k_{10}) \quad (5)$$

where k_7/k_8 is the dissociation constant of FQ, and k_9/k_{10} is the F ⇌ E equilibrium constant (*33*, *34*). Thus, from eq 5, K_{IQ}^{slope} contains only equilibrium terms. When $k_9 \ll k_{10}$, in an iso mechanism, the right side of eq 5 reduces to k_7/k_8. In contrast, K_{IQ}^{int} shows kinetic terms in addition to the equilibrium term k_7/k_8 (*34*):

$$K_{IQ}^{int} = k_7/k_8(1 + k_9/k_5 + k_9/k_3) + k_9/k_8 \quad (6)$$

consistent with the greater values of K_{IQ}^{int} than of K_{IQ}^{slope} for both 8-oxo-dGMP and dGMP (Table 1).

In the absence of Q, eq 4 reduces to one which shows uncompetitive product inhibition by P, where (*33*, *34*):

$$K_{IP}^{int} = k_5/k_6(1 + k_7/k_9 + k_7/k_3) + k_7/k_6 \quad (7)$$

In addition to k_5/k_6, which is the dissociation constant of P from the ternary product complex, eq 7 also contains three kinetic terms. Hence, in general, K_{IP}^{int} will exceed the true dissociation constant of P from the ternary product complex. Of the three kinetic terms in eq 7, one contains the rate constant (k_6) for the binding of P, and another contains the rate constant (k_3) of the chemical step in which P is formed. Hence, the 12-fold lowering of K_{IP}^{int} of PPi on replacing the Mg^{2+} activator with Mn^{2+} (Table 4) could have resulted from either a decrease in the dissociation constant of PPi (k_5/k_6), or an increase in k_3, the rate constant of the chemical step. As discussed above, the latter is less likely because k_{cat} with Mn^{2+} is 21-fold lower than with Mg^{2+} (*4*), and the k_3 step may contribute to k_{cat} (*6*).

$^1H-^{15}N$ HSQC Titrations of MutT with dGMP and 8-oxo-dGMP. To independently test the kinetic mechanism (Scheme 2) and the large differences in affinities of MutT for dGMP and 8-oxo-dGMP, direct binding studies of the nucleotide products to the Mg^{2+} complex of MutT were carried out. The effects of dGMP and 8-oxo-dGMP binding on the backbone ^{15}N and NH resonances of MutT were compared by $^1H-^{15}N$ HSQC titrations with these two nucleotides. In the presence of Mg^{2+}, the binding of dGMP resulted in stepwise changes in backbone ^{15}N and NH chemical shifts of 22 residues, distributed around the nucleotide binding site (Figure 5), indicating weak binding and fast exchange of the nucleotide on and off of the enzyme at a rate exceeding the chemical shift differences between those of the free and bound enzyme. The titration data for six residues which showed the largest changes in chemical shifts, V8, G9, N16, I20, V58, and E74, were fit to eq 2, assuming dGMP binding

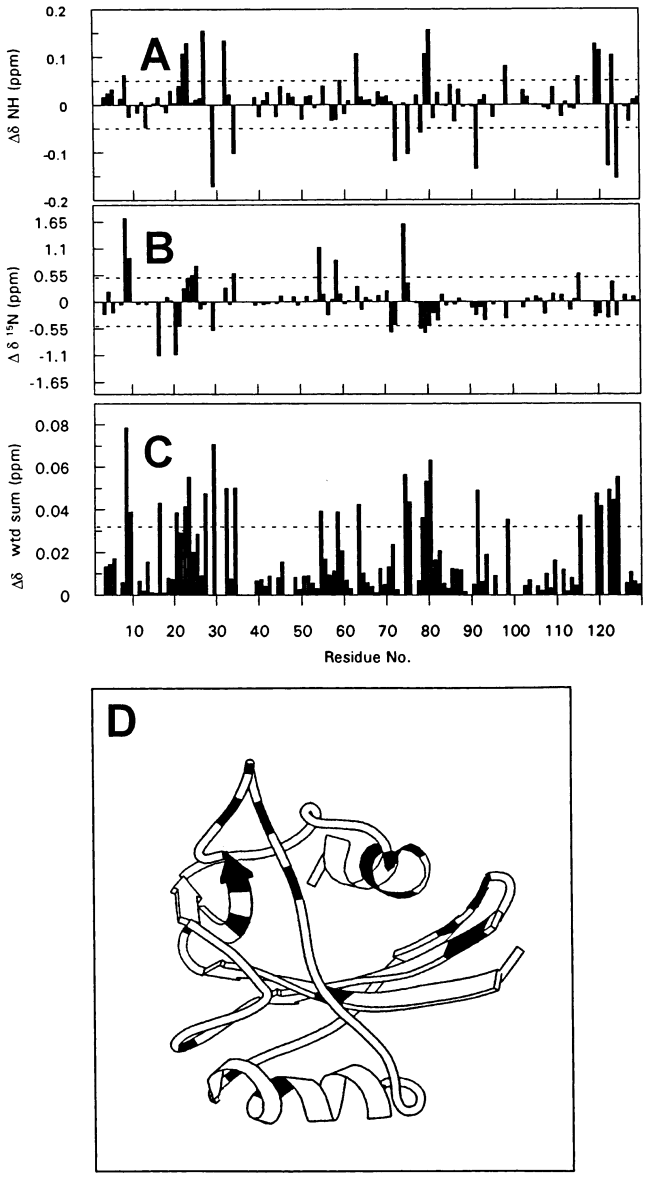

FIGURE 5: Backbone ^{15}N and NH chemical shift differences between the MutT−Mg^{2+}−dGMP and the MutT−Mg^{2+} complexes. Chemical shift differences ($\Delta\delta = \delta_{MutT-Mg^{2+}-dGMP} - \delta_{MutT-Mg^{2+}}$) were calculated on the basis of the chemical shift values obtained from $^1H-^{15}N$ HSQC spectra and are plotted vs residue number. (A) NH chemical shift differences. (B) ^{15}N chemical shift differences. (C) Sum of the absolute magnitudes of the ^{15}N and NH chemical shift changes which were weighted according to the backbone amide chemical shift dispersion in the ^1H (3.38 ppm) and ^{15}N (28.586 ppm) dimensions of the MutT−Mg^{2+} spectra. (D) Sites of backbone NH and/or ^{15}N chemical shift differences (twice the error limits) from MutT−Mg^{2+}−dGMP and MutT−Mg^{2+} are shaded in black. Samples contained 0.75 mM MutT, 15.0 mM $MgCl_2$, 21.0 mM NaCl, 0.33 mM NaN_3, 4.0 mM d_{11}-Tris-HCl, pH 7.5 (in 10% (v/v) D_2O). T = 23 °C.

to a single site on MutT−Mg^{2+}, yielding an average dissociation constant K_D = 1.79 ± 0.13 mM (Figure 6A). Attempts to fit the titration data to more than one binding site significantly increased the errors. Hence dGMP binds to the enzyme with a K_D in excellent agreement with its K_I^{slope} of 1.74 ± 0.48 mM (Table 5), as required by Scheme 2 for the product (Q) which leaves last.

The effects of 8-oxo-dGMP on the $^1H-^{15}N$ HSQC spectra of the MutT−Mg^{2+} complex were very different from those observed with dGMP (Figures 6B, 7, and 8). No stepwise

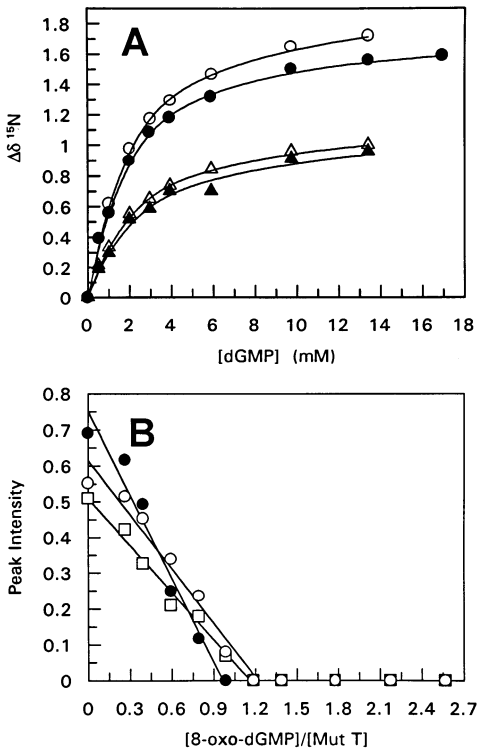

FIGURE 6: $^1H-^{15}N$ HSQC titrations of MutT with dGMP and 8-oxo-dGMP. (A) Determination of the K_D of dGMP in the presence of 0.75 mM MutT and 15.0 mM $MgCl_2$ by plotting ^{15}N chemical shift differences of V8 (○), E74 (●), N16 (△), and I20 (▲) vs dGMP concentration. Stoichiometric $MgCl_2$ was added with dGMP. Other components and conditions are as given in Figure 5. The titration data were fitted to eq 2, which yielded K_D values of 1.582, 1.509, 1.849, and 2.111 mM. A total of six titration curves were fitted, yielding an average K_D value of 1.79 ± 0.13 mM and a stoichiometry of 1.0. (B) Determination of binding stoichiometry of 8-oxo-dGMP to MutT. Plot of Peak intensity of F35 (●), Q55 (○), and T81(□) vs [8-oxo-dGMP]/[MutT] molar ratios. Peak intensities were obtained from HSQC titrations of MutT (0.25 mM) with 8-oxo-dGMP, in the presence of 15.0 mM $MgCl_2$ and at 23 °C. Other components and conditions were the same as those given in Figure 5.

Table 5: Comparison of Kinetically Determined Dissociation Constants with Those Measured by Direct Binding Studies at 23 °C

ligand	K_I^{slope} (μM)	K_D (μM)
dGMP	1740 ± 490	1790 ± 130[a]
8-oxo-dGMP	0.049 ± 0.015	0.052 ± 0.013[b]

[a] From $^1H-^{15}N$ HSQC titration. [b] From ITC.

changes in chemical shifts were seen. Rather, stepwise decreases in the intensities of 62 cross-peaks, together with the appearance of 62 new cross-peaks occurred with increasing concentrations of 8-oxo-dGMP, indicating the tight binding and slow exchange of this nucleotide. A sharp end point at a binding stoichiometry of 1.0 ± 0.1 nucleotide/enzyme was observed (Figure 6B). The dissociation constant could not be calculated because it was much lower than the concentration of the MutT enzyme (0.25 mM) required for this titration. Nonetheless, the tight binding of 8-oxo-dGMP to MutT with $K_D \ll 0.25$ mM, is consistent with the kinetic data (Table 1) and with Scheme 2 for the product (Q) which leaves last.

On the basis of the solution structure of the quaternary MutT−Mg^{2+}−(H_2O)−AMPCPP−Mg^{2+} complex (*5*), the AMP moiety of the nucleotide is in direct contact with only five residues of this 129 residue enzyme (L4, I6, K39, I80, and L82), and nine additional residues form a second shell (K2, Q5, E41, L71, Y73, F75, R78, T81, and N119). The 62 residues of MutT with backbone chemical shifts significantly altered by the binding of one molecule of 8-oxo-dGMP (Figure 8D) include all five of the residues in direct contact and five of the nine second shell residues (L71, Y73, R78, T81, and N119). They clearly cover much more surface area than that occupied by the bound nucleotide, indicating widespread structural changes in the enzyme, possibly tightening and closing down the active site around 8-oxo-dGMP. In contrast dGMP binding altered the backbone chemical shifts of only 22 residues surrounding the nucleotide binding site, including those of F75, I80, and N119 (Figure 5D). Figure 7, which directly compares the $^1H-^{15}N$ HSQC spectra of the MutT−Mg^{2+}−dGMP and MutT−Mg^{2+}−8-oxo-dGMP ternary complexes, clearly indicates the marked structural differences between them.

Isothermal Titration Calorimetry of the MutT−Mg^{2+}−8-oxo-dGMP Complex. Isothermal titration calorimetry was performed to verify the magnitude and nature of the high affinity of Mg^{2+}−MutT for 8-oxo-dGMP. As exemplified in Figure 9, each addition of 8-oxo-dGMP resulted in a significant release of heat. The data on two such experiments in Tris-HCl buffer at 23 °C were fit to yield an average K_D for 8-oxo-dGMP of 52 ± 13 nM, in excellent agreement with the K_I^{slope} of 49 ± 15 nM measured at the same temperature and in the same buffer (Tables 1, 5), indicating a $\Delta G^\circ_{binding}$ of −9.8 ± 0.2 kcal/mol. The K_D of 8-oxo-dGMP measured by ITC in HEPES buffer (65 ± 15 nM) also overlapped with these values.

Such ITC experiments, performed in two different buffers at pH 7.5, 50 mM HEPES and 50 mM Tris−HCl, in the presence of 15 mM $MgCl_2$, permitted the separation of the heat of binding ($\Delta H_{binding}$) from the heat of change in protonation of the buffer ($\Delta H_{ionization}$). With the experimental enthalpies of binding obtained in the two different buffers, eq 3 was used to solve for the change in protonation state (Δn) and the enthalpy of binding ($\Delta H_{binding}$). The experimental enthalpy of binding in the Tris−HCl buffer system was −28.2 ± 0.3 kcal/mol which overlaps with the $\Delta H_{binding}$ of −25.5 ± 4.1 kcal/mol obtained from the K_I^{slope} by the van't Hoff method in the same buffer. In HEPES buffer, the experimental enthalpy of binding obtained by ITC was −34.3 ± 0.6 kcal/mol. The enthalpies of ionization of Tris−HCl and HEPES buffers (corrected to 23 °C from their reported values at 25 °C using their reported ΔC_p values (*38*, *39*)) were 11.41 ± 0.02 (*38*) and 4.92 ± 0.02 kcal/mol (*39*), respectively. Using these values yielded a Δn of 0.95 ± 0.11 and an enthalpy of binding ($\Delta H_{binding}$) for 8-oxo-dGMP of −39.0 ± 0.7 kcal/mol at 23 °C. This value and the $\Delta G^\circ_{binding}$ of −9.8 ± 0.2 kcal/mol, yielded a calorimetric value for $-T\Delta S^\circ$ of +29.2 ± 0.7 kcal/mol at 23 °C (Table 3). From the literature, nucleotide binding to other proteins studied by ITC showed favorable values of $\Delta H_{binding}$ ranging from −3 to −69 kcal/mol and both unfavorable and favorable $-T\Delta S^\circ$ values (*40*, *41*).

The present calorimetric data are in qualitative agreement with the van't Hoff analysis of the kinetic data in that they both show that the binding of 8-oxo-dGMP to Mg^{2+}−MutT

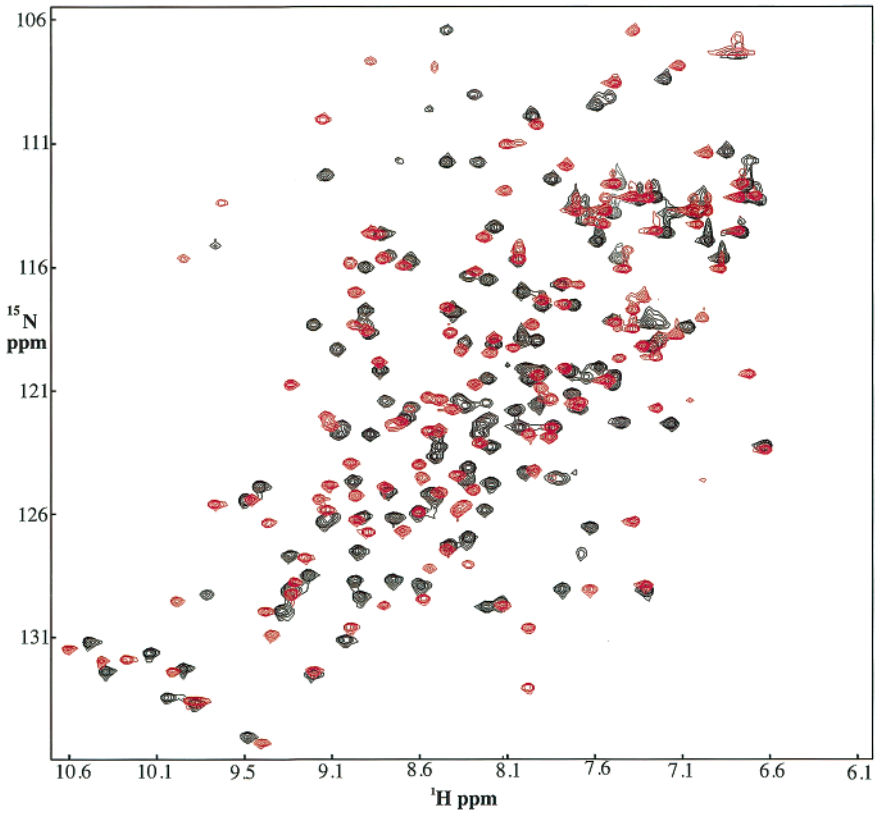

FIGURE 7: Comparison of ^{1}H−^{15}N HSQC spectra of the MutT−Mg^{2+}−dGMP complex (black) with that of the MutT−Mg^{2+}−8-oxo-dGMP complex (red). The MutT−Mg^{2+}−dGMP complex contained 0.75 mM MutT, 34.9 mM $MgCl_2$, and 16.9 mM dGMP. The MutT−Mg^{2+}−8-oxo-dGMP complex contained 0.25 mM MutT, 14.5 mM $MgCl_2$, and 0.29 mM 8-oxo-dGMP. Other components and conditions were the same as those given in Figure 5.

is enthalpically driven. The calorimetric enthalpy of binding at 23 °C (−39.0 ± 0.7 kcal/mol), however, is more negative than the van't Hoff enthalpy (−25.5 ± 4.1 kcal/mol). Attempts to improve the agreement by fitting the temperature dependence of K_I^{slope} to an expanded form of the van't Hoff equation which assumes that $\Delta H_{binding}$ varies with temperature (*42*, *43*) yielded poorly determined parameters with large errors. This difference in $\Delta H_{binding}$ may be due to the adjustment of the pH to 7.5 at each temperature in measuring the van't Hoff enthalpies or, more likely, to a significant change in heat capacity (ΔC_p) upon binding, which may affect van't Hoff enthalpies (*42*, *44*).

Accordingly, a ΔC_p of −680 ± 60 cal mol^{-1} K^{-1} was directly determined by calorimetric measurements of the $\Delta H_{binding}$ of 8-oxo-dGMP at three temperatures (*18*, *23*, and *28* °C) in Tris−HCl buffer by taking the slope of $\Delta H_{binding}$ versus *T* (data not shown). A negative change in heat capacity is generally believed to indicate the burial of hydrophobic groups (*43*). Such a change on binding of 8-oxo-dGMP to Mg^{2+}−MutT is consistent with the solution structure of the MutT−Mg^{2+}−(H_2O)−AMPCPP−Mg^{2+} complex (*5*), which shows the AMP moiety to be in direct contact with only five residues, at least four of which are hydrophobic (L4, I6, K39, I80, and L82). The site of protonation responsible for the Δn of 0.95 ± 0.11 on binding of 8-oxo-dGMP to MutT is unknown, but it may be on the phosphate, which would facilitate nucleotide interaction with a hydrophobic environment.

The $\Delta H_{binding}$'s of 8-oxo-dGMP obtained by the van't Hoff (−25.5 kcal/mol) and calorimetric (−39.0 kcal/mol) methods are both energetically highly favorable, while the corresponding values of $-T\Delta S^{\circ}_{binding}$ of +15.7 and +29.2 kcal/mol, respectively, are both highly unfavorable (Table 3). The favorable $\Delta H_{binding}$ may result from the slight tightening of numerous hydrogen bonds of the protein as it closes around the nucleotide, while the resulting increase in structural order could explain the unfavorable $-T\Delta S^{\circ}_{binding}$. Consistent with strengthened hydrogen bonding in the MutT−Mg^{2+}−8-oxo-dGMP complex, 28 (57%) of the 49 backbone NH resonances of MutT which shifted significantly on binding of 8-oxo-dGMP showed downfield proton shifts (Figure 8). Nine of these 28 residues were in α-helices, six were in *β*-strands, and 13 were in loops. In contrast, only 11 (65%) of the 17 backbone NH resonances of MutT that shifted significantly on dGMP binding, showed downfield proton shifts (Figure 5), suggesting shortening of NH hydrogen bonds of these residues. Three of these 11 residues were in α-helices, five were in *β*-strands, and three were in loops.

Isothermal Titration Calorimetry of the MutT−Mg^{2+}−dGMP Complex. For comparison, the $10^{4.6}$-fold weaker binding of dGMP to Mg^{2+}−MutT was studied by ITC in Tris-HCl buffer at 23 °C to determine the $\Delta H_{binding}$. Unlike the results with 8-oxo-dGMP, a net uptake of heat was observed with each addition of dGMP, dominated by the large endothermic heat of dilution of the nucleotide at the high levels required (0.3−4.9 mM) (data not shown). An accurate calorimetric measurement of K_D^{dGMP} could not be obtained because the low affinity of Mg^{2+}−MutT for dGMP would have required an enzyme concentration exceeding 2 mM, where aggregation occurs. However, the sign and approximate value of the $\Delta H_{binding}$ of dGMP could be obtained as follows. Correcting for the large positive heat

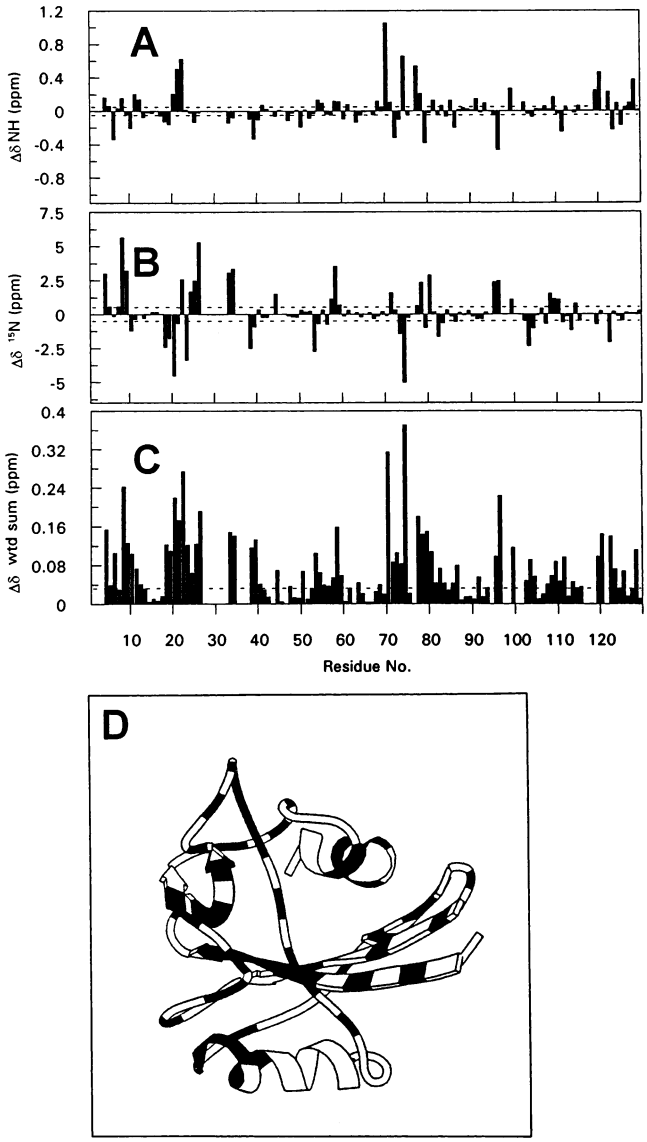

FIGURE 8: Backbone ^{15}N and NH chemical shift differences between the MutT−Mg^{2+}−8-oxo-dGMP and MutT−Mg^{2+} complexes. Chemical shift differences ($\Delta\delta = \delta_{MutT-Mg^{2+}-8-oxo-dGMP} - \delta_{MutT-Mg^{2+}}$) were calculated on the basis of the chemical shift values obtained from $^{1}H-^{15}N$ HSQC spectra and plotted vs residue number. (A) NH chemical shift differences. (B) ^{15}N chemical shift differences. (C) Sum of the absolute magnitudes of the ^{15}N and NH chemical shift changes which were weighted according to the backbone amide chemical shift dispersion in the ^{1}H and ^{15}N dimensions (3.38 and 28.586 ppm, respectively) of the MutT−Mg^{2+} spectra. The dashed lines indicate the error limits. (D) Sites of backbone NH and/or ^{15}N chemical shift differences (twice the error limits) from the MutT−Mg^{2+}−8-oxo-dGMP and MutT−Mg^{2+} complexes are shaded in black. Components and conditions are given in Figures 5 and 6.

of dilution of the nucleotide from direct measurements of it and using the average K_D^{dGMP} of 1.76 ± 0.49 mM, as found by both kinetics (K_I^{slope}) and NMR titration (Table 5), to determine the enzyme site occupancy by dGMP at each point in the titration curve, yielded a $\Delta H_{binding}$ for dGMP of −3.3 ± 0.3 kcal/mol. Since the $\Delta G°_{binding}$ of dGMP is −3.7 ± 0.3 kcal/mol at 23 °C, the entropic barrier to dGMP binding is probably negligible ($-T\Delta S°_{binding} = -0.4 \pm 0.4$ kcal/mol) (Table 3). Hence, the binding of both nucleotides is enthalpically driven, and the $10^{4.6}$-fold (or 6.1 kcal/mol) greater affinity of Mg^{2+}−MutT for 8-oxo-dGMP than for

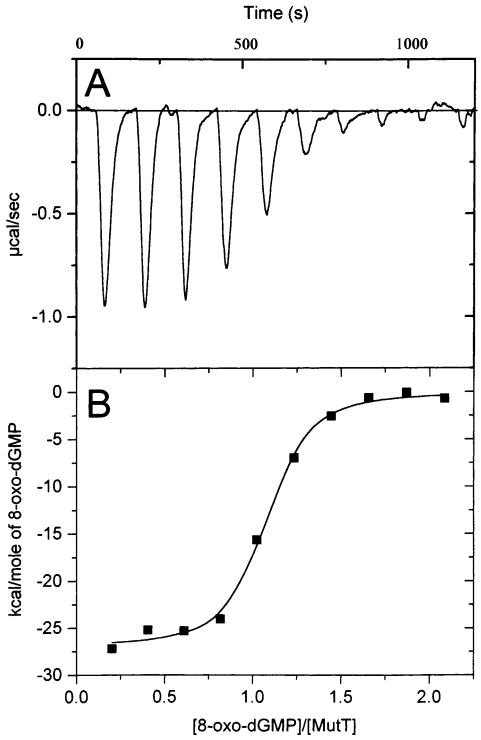

FIGURE 9: Determination of dissociation constant and enthalpy of binding of 8-oxo-dGMP to Mg^{2+}−MutT by isothermal titration calorimetry. (A) 1.8 mL of a solution of MutT (4.5 μM) containing 15 mM $MgCl_2$ and 50 mM Tris−Cl (pH 7.5) was titrated with 8-oxo-dGMP (123 μM), in 15 mM $MgCl_2$ and 50 mM Tris−Cl (pH 7.5) at 23 °C by adding 10 μL amounts of titrant every 120 s with a 20 s injection duration. (B) The association constant and enthalpy of binding of 8-oxo-dGMP to MutT were calculated by plotting heat of binding vs the mole ratio [8-oxo-dGMP]/[MutT] after subtracting the heat of dilution of the nucleotide, separately measured by adding the nucleotide to the buffer. The data are fit by assuming a single set of noninteracting sites with a $K_D^{8-oxo-dGMP}$ of 65 ± 12 nM and a $\Delta H_{experimental}$ of −27.0 ± 0.5 kcal/mol, where the errors represent one asymptotic standard error (45). An otherwise identical experiment, with a longer time between injections of 210 s, gave values which were not significantly different: a $K_D^{8-oxo-dGMP}$ of 39 ± 6 nM and a $\Delta H_{experimental}$ of −29.3 ± 0.4 kcal/mol, yielding average values of $K_D^{8-oxo-dGMP} = 52 \pm 13$ nM and $\Delta H_{experimental} = 28.2 \pm 1.2$ kcal/mol, respectively.

dGMP is a result of the much larger negative $\Delta H_{binding}$ of 8-oxo-dGMP.

CONCLUSIONS

Noncompetitive product inhibition of MutT by the nucleotides dGMP and 8-oxo-dGMP, uncompetitive inhibition by pyrophosphate, and direct nucleotide binding studies indicate an "iso" kinetic mechanism in which the pyrophosphate product dissociates first, followed by the nucleotide, leaving an altered form of the enzyme. This altered form reverts to the form which binds substrate in a partially rate-limiting step (Scheme 2).

Changing the metal activator from Mg^{2+} to Mn^{2+} had only small effects on the K_I values of the nucleotides but decreased the K_I of pyrophosphate 12-fold, consistent with direct coordination of the pyrophosphate product by the enzyme-bound divalent cation. A revised mechanism for MutT which takes all of these observations into account is given in Figure 10. The mechanism in Figure 10 differs from that in Figure 1 in that the PPi product leaves the enzyme first, displaced

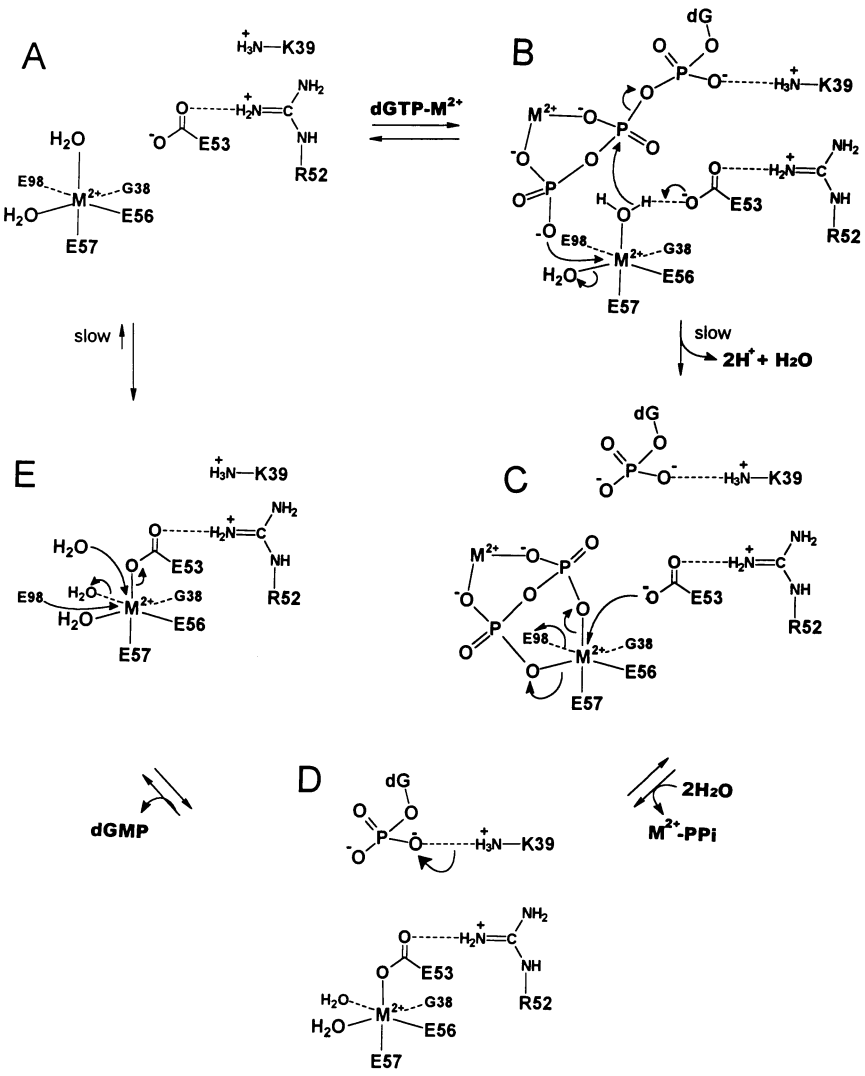

FIGURE 10: Revised mechanism of the MutT reaction taking into account the present studies of product inhibition and product binding and previous structural (*5*) and mutagenesis studies (*6*).

from the enzyme-bound divalent cation by Glu-53 (Figure 10C→D), followed by the nucleotide product (Figure 10D→E). The slow dissociation of Glu-53 from the enzyme-bound divalent cation prior to substrate binding (Figure 10E→A) constitutes the "iso" step. The chemical step (Figure 10B→C) and the dissociation of the nucleotide product (Figure 10D→E) may also be partially rate-limiting, especially in the case of 8-oxo-dGMP.

The present kinetic and direct binding studies establish the unusually high affinity of MutT for 8-oxo-dGMP, (K_I^{slope} = 49 nM; K_D = 52 nM), more than 10^4-fold greater than that for dGMP (K_I^{slope} = 1.7 mM; K_D = 1.8 mM) (Table 5). As found in studies of other nucleotide-protein interactions (*40*, *41*), the high affinity of MutT for 8-oxo-dGMP is the result of a favorable $\Delta H_{binding}$, which, in the present case, greatly exceeds the unfavorable $-T\Delta S^{\circ}_{binding}$. Sixty-two of the 129 residues of MutT, widely distributed throughout the protein, showed significant and large changes in chemical shifts of backbone ^{15}N and NH resonances in response to the binding of 8-oxo-dGMP. In contrast, in response to the binding of dGMP, only 22 residues surrounding the nucleotide binding site showed changes in chemical shifts, and these changes were smaller than those found with 8-oxo-dGMP. These findings indicate that the binding of 8-oxo-dGMP induces widespread structural changes in MutT, possibly closing down the active site. Such structural changes may include the strengthening of numerous backbone hydrogen bonds, explaining the favorable $\Delta H_{binding}$, while increasing the structural order of the protein, consistent with the unfavorable $\Delta S^{\circ}_{binding}$.

ACKNOWLEDGMENT

We are grateful to Dr. Jerry Hart, Dr. Jun Liu, and Dr. Phillip Cole for permitting us to use their FPLC and HPLC instruments and to Dr. Robert Cole for the mass spectral analysis. We also thank Dr. I. A. Rose, Dr. D. B. Northrop, and Dr. W. W. Cleland for advice on iso mechanisms.

SUPPORTING INFORMATION AVAILABLE

Two figures, Figure S1 showing MutT inhibition by 8-oxo-dGMP with Mn^{2+} as the activator, and Figure S2 showing MutT inhibition by dGMP with Mn^{2+} as the activator. This material is available free of charge via the Internet at http://pubs.acs.org.

REFERENCES

1. Bessman, M. J., Frick, D. N., and O'Handley, S. F. (1996) *J. Biol. Chem. 271*, 25059−25062.

2. Weber, D. J., Bhatnagar, S. K., Bullions, L. C., Bessman, M. J., and Mildvan, A. S. (1992) *J. Biol. Chem. 267*, 16939−16942.
3. Mildvan, A. S., Weber, D. J., and Abeygunawardana, C. (1999) *Adv. Enzymol. Relat. Areas Mol. Biol. 73*, 183−207.
4. Frick, D. N., Weber, D. J., Gillespie, J. R., Bessman, M. J., and Mildvan, A. S. (1994) *J. Biol. Chem. 269*, 1794−1803.
5. Lin, J., Abeygunawardana, C., Frick, D. N., Bessman, M. J., and Mildvan, A. S. (1997) *Biochemistry 36*, 1199−1211.
6. Harris, T. K., Wu, G., Massiah, M. A., and Mildvan, A. S. (2000) *Biochemistry 39*, 1655−1674.
7. Maki, H., and Sekiguchi, M. (1992) *Nature 355*, 273−275.
8. Shibutani, S., Takeshita, M., and Grollman, A. P. (1991) *Nature 349*, 431−434.
9. Cheng, K. C., Cahill, D. S., Kasai, H., Nishimura, S., and Loeb, L. A. (1992) *J. Biol. Chem. 267*, 166−172.
10. Treffers, H. P., Spinelli, V., and Belser, N. O. (1954) *Proc. Natl. Acad. Sci. U.S.A. 40*, 1064−1071.
11. Yanofsky, C., Cox, E. C., and Horn, V. (1966) *Proc. Natl. Acad. Sci. U.S.A. 55*, 274−281.
12. Kakuma, T., Nishida, J., Tsuzuki, T., and Sekiguchi, M. (1995) *J. Biol. Chem. 270*, 25942−25948.
13. Mo, J.-Y., Maki, H., and Sekiguchi, M. (1992) *Proc. Natl. Acad. Sci. U.S.A.* 89, 11021−11025.
14. Tsuzuki, T., Egashira, A., Igarashi, H., Iwakuma, T., Nakatsuru, Y., Tominaga, Y., Kawate, H., Nakao, K., Nakamura, K., Ide, F., Kura, S., Nakabeppu, Y., Katsuki, M., Ishikawa, T., and Sekiguchi, M. (2001) *Proc. Natl. Acad. Sci. U.S.A. 98*, 11456−11461.
15. Tassotto, M. L., and Mathews, C. K. (2002) *J. Biol. Chem. 277*, 15807−15812.
16. Mildvan, A. S., Saraswat, V., and Massiah, M. (2002) in *Proceedings of the 223rd National Meeting of American Chemical Society, Division of Physical Chemistry*, Orlando, FL, April 7−11, 2002, Abstract # 262, American Chemical Society, Washington, DC.
17. Abeygunawardana, C., Weber, D. J., Frick, D. N., Bessman, M. J., and Mildvan, A. S. (1993) *Biochemistry 32*, 13071−13080.
18. Nampalli, S., and Kumar, S. (2000) *Bioorg. Med. Chem. Lett. 10*, 1677−1679.
19. Kasai, H., and Nishimura, S. (1984) *Nucleic Acids Res. 12*, 2137−2145.
20. Trilink Biotechnologies, Inc., San Diego (1999) product data sheet.
21. Bhatnagar, S. K., Bullions, L. C., and Bessman, M. J. (1991) *J. Biol. Chem. 266*, 9050−9054.
22. Kay, L. E., Keifer, P., and Saarinen, T. (1992) *J. Am. Chem. Soc. 114*, 10663−10665.
23. Delaglio, F., Grzesiek, S., Vuister, G. W., Zhu, G., Pfeifer, J., and Bax, A. (1995) *J. Biomol. NMR 6*, 277−293.
24. Johnson, B. A., and Blevins, R. A. (1994) *J. Biomol. NMR 4*, 603−614.
25. Braunschweiler, L., and Ernst, R. R. (1983) *J. Magn. Res. 53*, 521−528.
26. Davis, D. G., and Bax, A. (1985) *J. Am. Chem. Soc. 107*, 2820−2821.
27. Marion, D., Driscoll, P. C., Kay, L. E., Wingfield, P. T., Bax, A., Gronenborn, A. M., and Clore, G. M. (1989) *Biochemistry 28*, 6150−6156.
28. Bax, A., and Ikura, M. (1991) *J. Biomol. NMR 1*, 99−104.
29. Grzesiek, S., and Bax, A. (1993) *J. Biomol. NMR 3*, 185−204.
30. Wiseman, T., Williston. S., Brandts, J. F., and Lin, J. N. (1989) *Anal. Biochem. 179*, 131−137.
31. Cleland, W. W. (1977) *Adv. Enzymol. 45*, 273−387.
32. Segal, I. H. (1975) in *Enzyme Kinetics*, pp 544−560, Wiley-Interscience, New York.
33. Rebholz, K. L., and Northrop, D. B. (1995) in *Methods Enzymol. 249*, Ed. Purich, D., pp 211−240.
34. Rebholz, K. L. (1993) *Enzymatic Iso Mechanisms*: *Alanine Racemase, Fumarase, and Aspartic Proteinases*, Doctoral Thesis, pp 65−76, University of Wisconsin, Madison, WI.
35. Dawson, R. M. C., Elliot, D. C., Elliot, W. H., and Jones, K. M. (1986) in *Data for Biochemical Research*, p 408, Oxford University Press, New York.
36. Rose, I. A. (1998) *Biochemistry 37*, 17651−8.
37. Rose, I. A. (1997) *Biochemistry 36*, 12346−54.
38. Bates, R. G., and Hetzer, H. B. (1961*) J. Phys. Chem. 65*, 667−671.
39. Fukuda, H., and Takahashi, K. (1998) *Proteins 33*, 159−166.
40. Forstner, M., Berger, C., and Wallimann, T. (1999) *FEBS Lett. 461*, 111−114.
41. Garnier, C., Lafitte, D., Tsvetkov, P. O., Barbier, P., Leclerc-Devin, J., Millot, J.-M., Briand, C., Makarov, A. A., Catelli, M. G., and Peyrot, V. (2002) *J. Biol. Chem. 277*, 12208−14.
42. Chaires, J. B. (1997) *Biophys. Chem. 64*, 15−23.
43. Sturtevant, J. M. (1977) *Proc. Natl. Acad. Sci., U.S.A. 74*, 2236−2240.
44. Horn, J. R., Brandts, J. F., and Murphy, K. F. (2002) *Biochemistry 41*, 7501−7507.
45. Johnson, M. L. and Faunt, L. M. (1992) *Methods Enzymol. 210*, 1−37.

BI020552P